The Plant Cell, Vol. 27: 3277–3289, November 2015, www.plantcell.org

Septin-Dependent Assembly of the Exocyst Is Essential for Plant Infection by *Magnaporthe oryzae*[OPEN]

Yogesh K. Gupta,[a,b] Yasin F. Dagdas,[a,b] Ana-Lilia Martinez-Rocha,[a,1] Michael J. Kershaw,[a] George R. Littlejohn,[a] Lauren S. Ryder,[a] Jan Sklenar,[b] Frank Menke,[b] and Nicholas J. Talbot[a,2]

[a] School of Biosciences, University of Exeter, Exeter EX4 4QD, United Kingdom
[b] The Sainsbury Laboratory, Norwich NR4 7UH, United Kingdom

ORCID IDs: 0000-0002-8696-9044 (Y.K.G.); 0000-0002-9502-355X (Y.F.D.); 0000-0002-6560-3473 (A.-L.M.-R.); 0000-0002-8768-2598 (G.R.L.); 0000-0003-0370-5746 (L.S.R.); 0000-0003-1858-2574 (J.S.); 0000-0003-2490-4824 (F.M.); 0000-0001-6434-7757 (N.J.T.)

***Magnaporthe oryzae* is the causal agent of rice blast disease, the most devastating disease of cultivated rice (*Oryza sativa*) and a continuing threat to global food security. To cause disease, the fungus elaborates a specialized infection cell called an appressorium, which breaches the cuticle of the rice leaf, allowing the fungus entry to plant tissue. Here, we show that the exocyst complex localizes to the tips of growing hyphae during vegetative growth, ahead of the Spitzenkörper, and is required for polarized exocytosis. However, during infection-related development, the exocyst specifically assembles in the appressorium at the point of plant infection. The exocyst components Sec3, Sec5, Sec6, Sec8, and Sec15, and exocyst complex proteins Exo70 and Exo84 localize specifically in a ring formation at the appressorium pore. Targeted gene deletion, or conditional mutation, of genes encoding exocyst components leads to impaired plant infection. We demonstrate that organization of the exocyst complex at the appressorium pore is a septin-dependent process, which also requires regulated synthesis of reactive oxygen species by the NoxR-dependent Nox2 NADPH oxidase complex. We conclude that septin-mediated assembly of the exocyst is necessary for appressorium repolarization and host cell invasion.**

INTRODUCTION

Magnaporthe oryzae is a filamentous fungus and the causal agent of rice blast disease. Each year, rice blast disease causes up to 18% yield losses and recurrent epidemics occur in all rice-growing regions of the world (Wilson and Talbot, 2009). Understanding the biology of plant infection by *M. oryzae* is therefore critical for development of durable control strategies for blast disease. In order to infect plants, *M. oryzae* develops a specialized infection structure called an appressorium. This dome-shaped cell generates enormous turgor of up to 8.0 MPa to breach the leaf cuticle using a narrow penetration peg that develops from the base of the appressorium (de Jong et al., 1997; Wilson and Talbot, 2009). The fungus subsequently colonizes host epidermal cells and spreads rapidly in plant tissue. Appressorium development occurs in response to the hard, hydrophobic rice (*Oryza sativa*) leaf surface (Veneault-Fourrey et al., 2006; Saunders et al., 2010). The appressorium generates pressure by accumulating osmolytes, such as glycerol, to very high concentrations and uses autophagic cell death of the conidium to recycle cellular components to the developing appressorium (Veneault-Fourrey et al., 2006; Kershaw and Talbot, 2009).

Recently, it has been shown that septins assemble into a heteromeric ring at the point of plant infection, called the appressorium pore, where they scaffold a toroidal F-actin network at the base of the appressorium (Dagdas et al., 2012). Septin GTPases act as a diffusion barrier to localize Bin-Amphiphysin-Rvs (BAR)-domain proteins, required for generation of membrane curvature and protrusion of the penetration peg to rupture the leaf cuticle (Dagdas et al., 2012). Septin-mediated reorientation of F-actin is regulated by the action of NADPH oxidases (Nox), which generate reactive oxygen species in the appressorium (Ryder et al., 2013). The Nox2-NoxR complex is required for organization of the septin ring and F-actin network at the appressorium pore.

During plant infection, pathogenic fungi secrete a repertoire of small effector proteins to overcome plant immunity. *M. oryzae* secretes apoplastic effectors that localize at the plant fungal interface, while cytoplasmic effectors are expressed at a specialized plant-derived structure called the biotrophic interfacial complex and then delivered into rice cells (Khang et al., 2010). It has recently been shown that the *M. oryzae* exocyst subunits (Exo70 and Sec5) and the t-SNARE, Sso1, are required for secretion of cytoplasmic effectors (Giraldo et al., 2013; Giraldo and Valent, 2013).

In this report, we investigated the organization and function of the exocyst complex during plant infection by *M. oryzae*. Polarized exocytosis is an essential process in fungi required for cell growth, cell migration, and morphogenesis. Secretory vesicles are delivered to the hyphal tip and form a vesicle dense region, called the Spitzenkörper (Steinberg, 2007; Read, 2011; Sudbery, 2011b; Riquelme, 2013; Riquelme et al., 2014). This acts as a vesicle supply center, directing secretory vesicles for cell wall biogenesis to the hyphal tip (Riquelme et al., 2007; Verdín et al., 2009). The Spitzenkörper, together with the polarisome and exocyst complex,

[1] Current address: Department of Molecular Phytopathology and Genetics, University of Hamburg, Biozentrum Klein Flottbek, D-22609 Hamburg, Germany.
[2] Address correspondence to n.j.talbot@exeter.ac.uk.
The author responsible for distribution of materials integral to the findings presented in this article in accordance with the policy described in the Instructions for Authors (www.plantcell.org) is: Nicholas J. Talbot (n.j.talbot@exeter.ac.uk).
[OPEN]Articles can be viewed online without a subscription.
www.plantcell.org/cgi/doi/10.1105/tpc.15.00552

play a crucial role in hyphal tip growth (Taheri-Talesh et al., 2008; Sudbery, 2011a). In the budding yeast *Saccharomyces cerevisiae*, the polarisome complex consists of Peanut Shmoo 2, Spindle Pole Antigen 2 (Spa2), and the formin Bud Neck Involved 1, which nucleates F-actin cables to sites of polarized growth (Sheu et al., 1998; Sagot et al., 2002; Evangelista et al., 2003). Post-Golgi secretory vesicles are then delivered to the tip via the Rab GTPase Sec4, which is activated through its guanine nucleotide exchange factor (GEF), Sec2 (Stalder et al., 2013), and binds to the exocyst complex through Sec15 interaction (Salminen and Novick, 1989). The exocyst complex is an evolutionarily conserved octameric protein complex, comprising Sec3p, Sec5p, Sec6p, Sec8p, Sec10p, Sec15p, Exo70p, and Exo84p required for vesicle docking to the plasma membrane (TerBush et al., 1996; Guo et al., 1999; He and Guo, 2009). Vesicle fusion to the plasma membrane then requires v-SNAREs on vesicles and t-SNAREs at the plasma membrane (Novick et al., 2006).

Here, we show that the octameric exocyst complex in *M. oryzae* is located at the hyphal tip, ahead of the Spitzenkörper. During initial stages of appressorium development, the exocyst is located at the tips of germ tubes, but then adopts a cortical pattern of localization in the expanding appressorium, before specifically localizing to the appressorium pore. We demonstrate that exocyst assembly is dependent on septins, which facilitate cuticle rupture and plant infection by the fungus.

RESULTS

Subcellular Localization of Polarity Components in Vegetative Hyphae of *M. oryzae*

To understand the role of the exocyst during polarized, hyphal growth in *M. oryzae*, we visualized a range of polarity markers and each of the predicted exocyst components by tagging them with fluorescent proteins and expressing the functional constructs in *M. oryzae*. We first identified *M. oryzae* homologs of each gene by analysis of the genome sequence of *M. oryzae* (Dean et al., 2005), as shown in Supplemental Table 1. Each gene fusion was expressed under its native promoter in *M. oryzae* with C-terminal fusions of GFP used, except for Snc1, Cdc42, Rac1, and Sec4, where N-terminal GFP tags were generated.

We first observed localization of each of the exocyst components Exo70, Sec15, Sec8, Sec3, Sec6, Exo84, Sec5, and Sec10, in growing hyphae of *M. oryzae*. All exocyst components, except Sec10, localized to a crescent structure at the growing hyphal tip, as shown in Figure 1. We were unable to observe any signal in Sec10-GFP-expressing strains of *M. oryzae*. This is consistent with a previous finding in *Neurospora crassa*, where a Sec10-GFP fusion could not be localized, even though Sec10 was shown by immunoprecipitation to be part of the exocyst complex (Riquelme et al., 2014). This suggests that there might be a conserved structural impediment to expressing a Sec10-GFP fusion in the related ascomycete species, *M. oryzae* and *N. crassa*. Expression analysis of genes expressing each exocyst component was performed using SuperSAGE (Soanes et al., 2012) and suggested that *SEC10* is expressed in mycelium grown in complete medium and during appressorium development, albeit at a low level compared with some of the other exocyst components, such as *SEC3* and *SEC15* (Supplemental Figure 1).

To investigate location of the Spitzenkörper in *M. oryzae*, we labeled hyphae expressing exocyst-GFP fusions with the lipophilic styryl dye FM4-64 (Fischer-Parton et al., 2000). The Spitzenkörper appeared as a bright spot in the center of

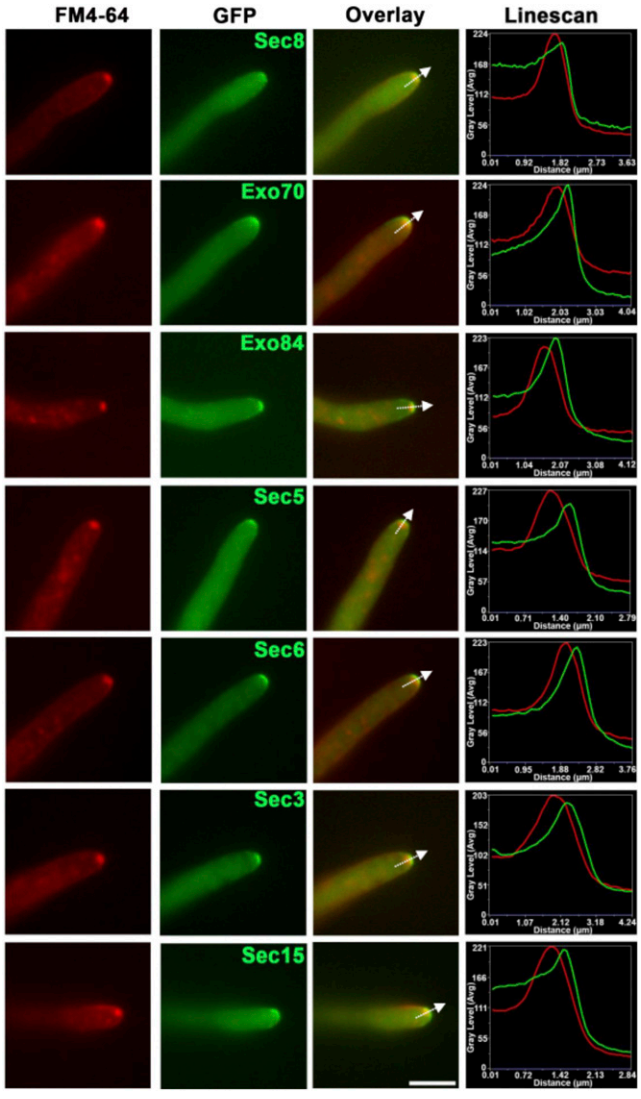

Figure 1. Localization of the Exocyst Complex in Vegetative Hyphae of *M. oryzae*.

Micrographs and corresponding line scan graphs to show localization of the exocyst complex and the Spitzenkörper in growing hyphae of *M. oryzae*. Strains of the fungus expressing Sec8-GFP, Exo70-GFP, Exo84-GFP, Sec5-GFP, Sec6-GFP, Sec3-GFP, and Sec15-GFP were prepared with each gene fusion expressed under control of its native promoter. Each strain was incubated overnight at 24°C on a 0.8% distilled water agar slide in a humid chamber. The lipophilic dye FM4-64 was then used to label the Spitzenkörper. Epifluorescence micrographs were overlaid to observe relative localization and a line scan graph generated at position shown by arrow to show FM4-64 (red) and GFP fluorescence (green). Bar = 10 μm.

the apical dome, while the exocyst components formed a surface crescent at the tips of cells (Figure 1; Supplemental Figure 2). Line scans of the fluorescence signals confirmed this separation for each component of the exocyst complex, with only a partial overlap in fluorescence observed, for example, with Sec3 (Supplemental Figure 2). By contrast, myosin light chain, Mlc1, localized to a region consistent with the Spitzenkörper (Supplemental Figure 3A). The polarisome component Spa2-GFP also localized as a bright spot at the hyphal tip (Supplemental Figure 3B and Supplemental Movie 1). Fimbrin-GFP localized subapically to a cortical collar in growing hyphae (Supplemental Figure 3C and Supplemental Movie 2), while other polarity components, Snc1, Sec2, Sec9, Sec4, and Rac1, preferentially localized to the tips of growing vegetative hyphae (Supplemental Figures 3D to 3H and Supplemental Movie 4). GFP-Cdc42 was cortically distributed with strong tip localization (Supplemental Figure 3I and Supplemental Movie 3). Moreover, Sec2, the putative GEF for Sec4, was tip localized, often appearing slightly subapical to the Spitzenkörper (Supplemental Figure 4) We conclude that the exocyst forms a complex at the very apex of hyphal tips of *M. oryzae* that is distinct from the Spitzenkörper.

To determine the composition of the exocyst complex, Sec6-GFP and Exo84-GFP were immunoprecipitated from hyphal protein extracts and liquid chromatography-tandem mass spectrometry (LC-MS/MS) performed to identify unique peptides. Mass spectrometry data were aligned with the predicted set of *M. oryzae* proteins and parameters set to 95% confidence for protein match and a minimum of two unique peptide matches with 95% confidence. All seven of the remaining exocyst subunits were identified by coimmunoprecipitation with Sec6 and Exo84, as shown in Table 1, consistent with the predicted octameric nature of the complex. Interestingly, Sec10 was always observed in coimmunoprecipitation experiments with both Sec6 and Exo84, and we conclude that it forms part of the octameric exocyst complex. However, our inability to colocalize Sec10 in live-cell imaging studies does not preclude the possibility that it is not always associated with the rest of the subunits or is present in only a subset of complexes. We also identified additional interacting proteins, including all four core septin GTPases, actin binding proteins, Rho-GTPase, and the Pmk1 MAPK (mitogen-activated protein kinase), which regulates appressorium development in *M. oryzae* (Xu and Hamer, 1996). The proteins identified are consistent with the exocyst being associated with the polarized tips of fungal hyphae and their predicted function in exocytosis, but also suggested a specific involvement in appressorium-mediated plant infection.

Organization of the Exocyst at the Appressorium Pore of *M. oryzae*

To understand the role of the exocyst components during plant infection, we visualized expression and localization of exocyst-GFP fusion proteins during a time course of appressorium development. Each exocyst subunit initially localized to tips of germinating conidia and germ tubes during the early stages of appressorium development, as shown in Figure 2 and Supplemental Figure 5. Once the appressorium formed, we observed exocyst components at the cortex of cells with a punctate distribution (4 to 8 h). In three-dimensional projections, it was clear that localization was associated with the base of the infection cell at its interface with the underlying surface (Supplemental Movie 6). In mature appressoria (24 h), exocyst components localized to a 4.0-μm-diameter ring (±0.4, n = 50) at the appressorium pore (Figures 2A and 2B; Supplemental Figure 5). This is consistent with the inside edge of the heteromeric septin ring complex and the toroidal F-actin network that brings about repolarization of the appressorium during plant infection (Dagdas et al., 2012). We colocalized F-actin in a strain expressing Sec6-GFP by expression of LifeAct-RFP. Toroidal F-actin colocalized with the exocyst ring extending in a larger, more dispersed network around the appressorium pore (Figure 2C). To investigate the nature of the appressorium pore, we investigated the localization of other polarity components. We found that Sec9-GFP, a putative membrane-bound t-SNARE, localized in puncta around the appressorium pore (Supplemental Figure 6). Similarly, Snc1-GFP (a putative vesicle-bound v-SNARE), Fim1-GFP (Fimbrin, an actin binding protein), Rac1-GFP (a Rho-type GTPase), and Cdc42-GFP (a polarity-associated small GTPase) all localized at the center of the appressorium pore (Supplemental Figure 6). These results are consistent with the appressorium pore acting as an active hub for signaling during reestablishment of polarized growth during plant infection.

Exocyst-Dependent Secretion at the Appressorium Pore

To investigate the role of the appressorium pore in polarized exocytosis, we next determined if known pathogenicity determinants are secreted in an exocyst-dependent manner during plant infection. We initially checked secretion of total protein in axenic culture from exocyst mutants Δ*sec5* and Δ*exo70* and compared this to the isogenic wild-type Guy11. In Δ*sec5* and Δ*exo70*, there was >50 and 60% reduction, respectively, in secretion of protein compared with Guy11 ($P < 0.01$) (Supplemental Figure 7). We then investigated secretion of a virulence-associated factor. During initiation of plant infection by *M. oryzae*, the fungal spore releases spore tip mucilage (STM) to attach itself to the leaf surface (Hamer et al., 1988). This acts as an adhesive and is also secreted from the appressorium to facilitate adhesion to the hydrophobic cuticle. STM can be detected using the lectin concanavalin A (ConA) conjugated to fluorescein isothiocyanate (FITC) (Hamer et al., 1988). We investigated STM secretion in Δ*sec5* and Δ*exo70* mutants. Spores from Δ*sec5* and Δ*exo70* mutants were harvested and appressoria allowed to form on hydrophobic borosilicate glass cover slips. Secretion of STM was then observed by FITC-ConA labeling and epifluorescence microscopy, as shown in Figure 3. Spores of Guy11 showed a very strong signal for STM compared with those of Δ*sec5* and Δ*exo70* mutants both at the tips of germinating conidia and at the base of appressoria (Figure 3A). We observed that 83 and 71% conidia from Δ*sec5* and Δ*exo70* mutants showed less fluorescence than Guy11, respectively (Figure 3B). Similarly, the fluorescence signal from mature appressoria in exocyst mutants was also significantly reduced ($P < 0.05$) with 80 and 66% of appressoria showing less fluorescence in Δ*sec5* and Δ*exo70* mutants, respectively, than Guy11.

Consistent with impaired secretion, Δ*sec5* and Δ*exo70* mutants are required for full virulence (Figures 3C and 3D). We used the susceptible rice cultivar Co-39 and found a significant ($P < 0.05$)

Table 1. Putative Exocyst-Interacting Proteins in *M. oryzae* Identified by Coimmunoprecipitation of *SEC6* and *EXO84*

M. oryzae Proteins Identified by Coimmunoprecipitation		Total Spectral Count/Total Protein Coverage (%)		
		Sec6:GFP	Exo84:GFP	Control
Exocyst	Sec3 (MGG_03323)	164/35	69/25	0/0
	Sec5 (MGG_07150)	35/29	57/48	0/0
	Sec6 (MGG_03235)	100/55	27/34	0/0
	Sec8 (MGG_03985)	153/61	48/42	0/0
	Sec10 (MGG_04559)	9/13	119/64	0/0
	Sec15 (MGG_00471)	7/11	77/54	0/0
	Exo70 (MGG_01760)	11/14	163/83	0/0
	Exo84 (MGG_06098)	10/13	191/86	0/0
Septins	Sep6 (MGG_07466)	2/12	1/2	0/0
	Sep4 (MGG_06726)	0/0	10/27	0/0
	Sep3 (MGG_01521)	2/3	0/0	0/0
	Sep5 (MGG_03087)	0/0	2/5	0/0
Actin binding	Fim1 (MGG_04478)	2/5	3/5	0/0
	Vps1/Dynamin (MGG_09517)	2/3	0/0	1/1
Rho-GTPase	Rho1 (MGG_07176)	8/22	2/16	0/0
	Rac1 (MGG_02731)	3/19	0/0	0/0
MAPK signaling pathway	Mst7 (MGG_06482)	6/3	8/3	1/0
	Pmk1 (MGG_09565)	2/5	6/19	0/0
	Mps1 (MGG_04943)	3/10	0/0	0/0
Others	Sec14 (MGG_00905)	2/17	4/12	0/0
	Sec26 (MGG_06860)	4/6	1/1	1/0
	Ypt1 (MGG_06962)	6/37	1/6	0/0
	Sec24 (MGG_09564)	3/3	1/1	0/0
	Sec63 (MGG_05320)	2/2	0/0	0/0
	Arb1(ABC transporter) (MGG_11862)	5/5	2/1	0/0
	Hex1 (Woronin body protein) (MGG_02696)	9/75	2/5	0/0

reduction in the ability of exocyst mutants to cause rice blast disease compared with Guy11 (Figure 3C). Taken together, we conclude that the appressorium pore is an active site of secretion during plant infection.

Sec6 Is Required for Exocyst Assembly at the Appressorium Pore

To investigate exocyst function, we attempted to generate targeted gene deletion mutants for all exocyst-encoding genes. All exocyst subunits are essential in yeast, except Sec3, although Δ*sec3* mutants show severe growth defects (Wiederkehr et al., 2003), while temperature-sensitive mutations in exocyst subunits lead to accumulation of secretory vesicles at the sites of bud tips and the mother bud neck (Novick et al., 1980). In *M. oryzae*, only Δ*sec5* and Δ*exo70* mutants could be generated (Giraldo et al., 2013). We therefore generated a temperature-sensitive mutant of *SEC6*. In yeast, the *sec6-4* mutant grows normally at 25°C, but at a nonpermissive temperature, 37°C, its growth is severely impaired. Generating a point mutation, L633P, in the *SEC6* coding region leads to the *sec6-4* phenotype (Lamping et al., 2005), so we attempted to target the same region of *M. oryzae SEC6* to generate a temperature-sensitive mutant by allelic replacement. We mutated the Y601P site in the *SEC6* coding region and then introduced the allele into *M. oryzae* by homologous recombination. Putative *sec6*^{Y601P} transformants were selected and showed a growth defect at a semirestrictive temperature of 29°C. Growth was restored by subsequent incubation at 24°C, as shown in Figure 4. Positive transformants were confirmed by DNA sequence analysis of the mutation site (Supplemental Figure 8B). Integration of the selectable maker hygromycin (1.4 kb) was further confirmed by PCR using primers Sec6.TS.2F and Sec6.30.1 (Supplemental Figure 8C and Supplemental Table 2).

In budding yeast, conditional mutation of Sec6 causes disassembly of the exocyst complex at 37°C (Songer and Munson, 2009). To test whether the exocyst complex depends on Sec6 for assembly at the appressorium pore, we investigated pore organization in the *sec6*^{Y601P} mutant. We localized Sec5-GFP and Sec8-GFP in the *sec6*^{Y601P} mutant and found that ring conformation of the exocyst complex was disrupted at the semirestrictive temperature of 29°C, but formed normally at 24°C (Figures 4B and 4C). Consistent with loss of exocyst organization, we found the *sec6*^{Y601P} mutant was significantly reduced ($P < 0.05$) in its ability to cause rice blast disease at 29°C, but showed normal virulence at 24°C compared with Guy11 (Figures 4D and 4E). We also localized exocyst components Exo70, Sec3, Exo84, and Sec15 in a *sec6*^{Y601P} mutant and none formed rings at 29°C (Supplemental Figure 9). Loss of virulence was restored when we complemented the *sec6*^{Y601P} mutant with a functional Sec6-GFP

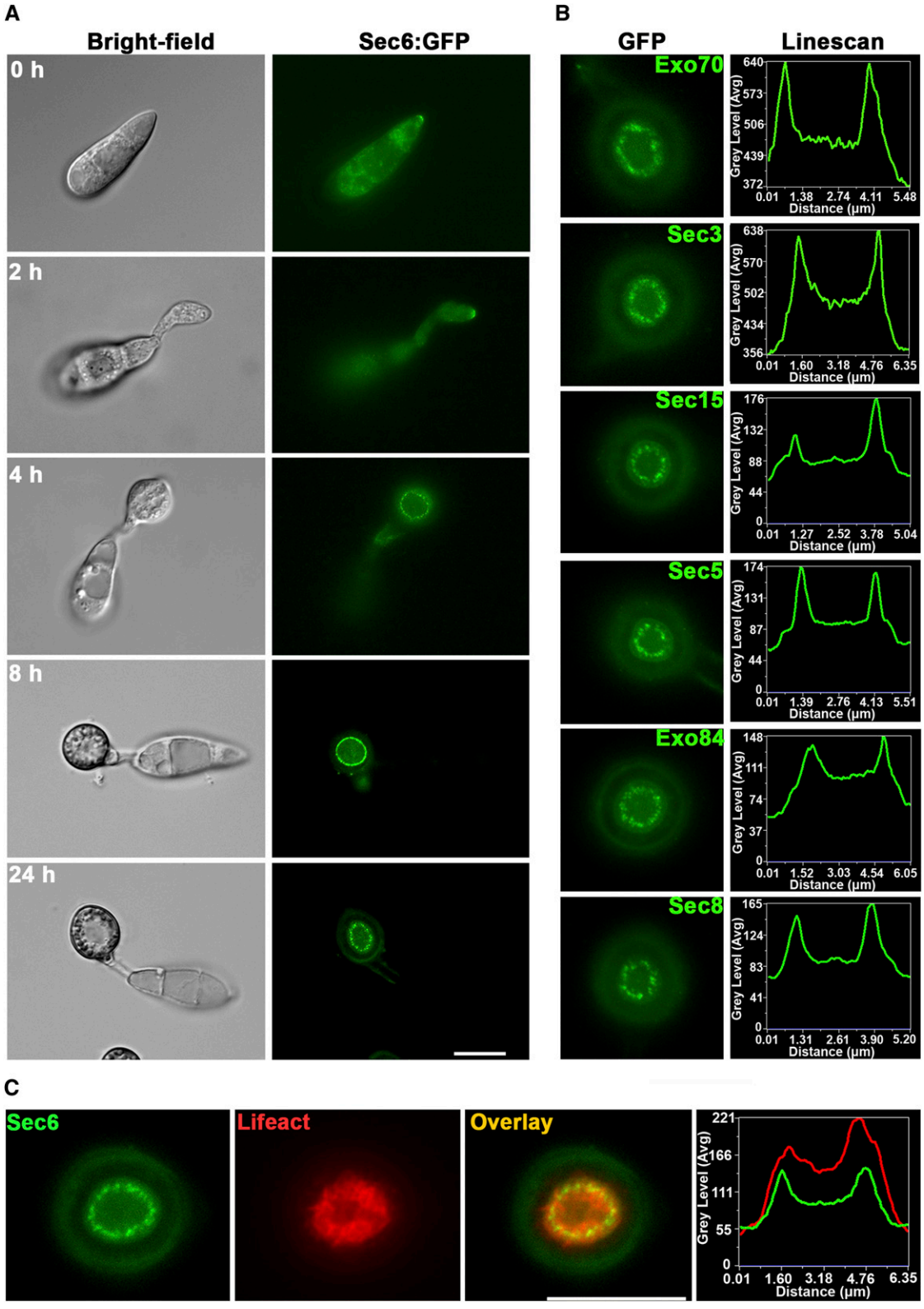

Figure 2. Expression of *M. oryzae* Exocyst Subunits during Appressorium Development.

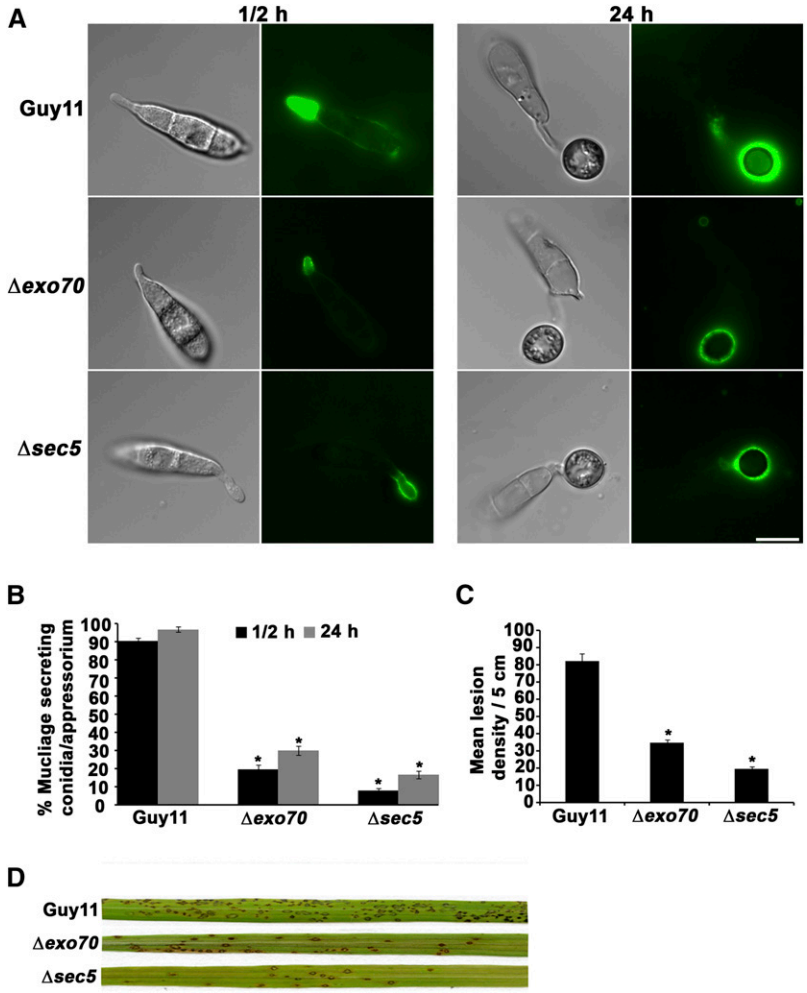

Figure 3. Exocyst Subunits Are Required for Secretion of Spore Tip Mucilage during Plant Infection.

(A) Mucilage secreted form the conidia stained with FITC-ConA. The conidial suspension of 5×10^4 mL^{-1} from wild-type Guy11, Δ*exo70*, and Δ*sec5* mutant strains were inoculated onto glass cover slips. Conidia from all the strains were stained with FITC-ConA after half an hour and 24 h of inoculation. Bar = 10 μm.
(B) Bar chart showing percentage of conidia/appressorium strongly labeled with FITC-ConA after half an hour (black bars) and 24 h (gray bars). Values are mean ± SD for three repetitions of the experiment, $n = 300$. Asterisk indicates significant difference at $P < 0.05$.
(C) Bar chart showing number of lesions per 5 cm on susceptible rice cultivar Co-39 sprayed with Guy11, Δ*exo70*, and Δ*sec5* mutant strains (*$P < 0.05$ for all mutants, $n = 30$ for each strain, mean ± SD, three experiments).
(D) Conidial suspension of 5×10^4 mL^{-1} from Guy11, Δ*exo70*, and Δ*sec5* mutant were sprayed on 3-week-old seedlings of susceptible rice cultivar Co-39. Disease symptoms were quantified after 5 d of incubation in a growth chamber, and a representative leaf from each infection is shown.

fusion (Supplemental Figure 8D). A leaf sheath assay was performed to check growth of invasive hyphae on rice cultivar Co-39. At semirestrictive temperature, the growth of the *sec6*^{Y601P} mutant is restricted in the first rice cell (45 h postinoculation), while Guy11, and complemented strains, invaded up to three rice cells by this time (Supplemental Figure 8D). We conclude that Sec6 is required for core assembly of exocyst subunits at the appressorium pore, which is a necessary prerequisite for plant infection.

Figure 2. (continued).

(A) *M. oryzae* Sec6 expressed with C-terminal GFP fusion under native promoter. During initial stages of conidial germination and germ tube formation, Sec6 localized to the germ tube tip and during early stages of appressorium formation Sec6-GFP localized to the periphery of the appressorium at the plasma membrane. After 24 h, Sec6 expressed at the base of the appressorium and formed a ring at the appressorial pore.
(B) Micrographs of the other exocyst subunits Exo70, Sec5, Exo84, Sec8, Sec3, and Sec15, which formed a ring at the appressorium pore after 24 h. Transverse line scan graphs show position exocyst-GFP fluorescence signal in the appressorium.
(C) Colocalization of Sec6-GFP and LifeAct-RFP in the mature appressorium and line scan graph consistent with colocalization of the exocyst ring and actin network around the appressorial pore. Bar = 10 μm.

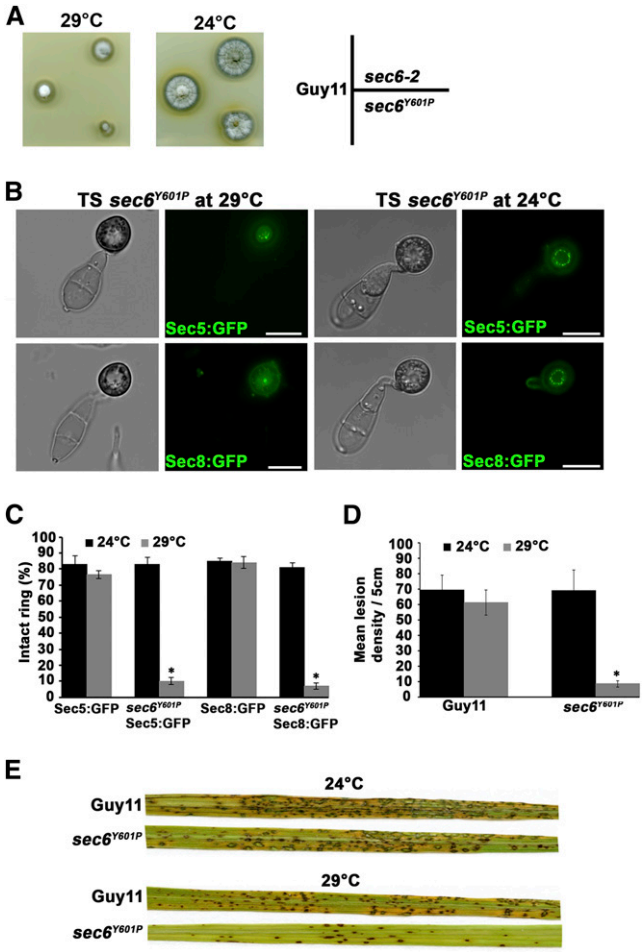

Figure 4. Sec6 Is Necessary for Exocyst Assembly at the Appressorium Pore.

(A) Temperature sensitivity of the *sec6*^{Y601P} mutant was tested by comparison of hyphal growth of an ectopic transformant (*sec6-2*) and wild-type Guy11 after incubation at the semirestrictive temperature of 29°C for 4 d and restoration of hyphal growth was done by incubation for a further 3 d at 24°C.

(B) Micrographs showing localization of exocyst subunits Sec5:GFP and Sec8:GFP in the temperature-sensitive mutant *sec6*^{Y601P} at a permissive temperature of 24°C and semirestrictive temperature of 29°C. Exocyst ring was completely mislocalized at the semirestrictive temperature of 29°C in the *sec6*^{Y601P} mutant. Bar = 10 μm.

(C) Bar chart showing percentage of appressoria expressing exocyst subunit Sec5:GFP and Sec8:GFP at the permissive temperature of 24°C (black bars) and semirestrictive temperature of 29°C (gray bars). Values are mean ± SD for three repetitions of the experiment, $n = 300$.

(D) Bar chart showing number of lesions per 5 cm on susceptible rice cultivar Co-39 sprayed with the wild-type Guy11 and temperature-sensitive mutant *sec6*^{Y601P} strains at a permissive temperature of 24°C (black bars) and semirestrictive temperature of 29°C (gray bars) ($P < 0.05$ for all mutants, $n = 30$ for each strain, mean ± SD, three experiments).

(E) *sec6*^{Y601P} mutant and Guy11 were sprayed on 3-week-old seedlings of susceptible rice cultivar Co-39 with a conidial concentration of 5×10^4 mL^{-1} and incubated for 5 d at the permissive temperature of 24°C and semirestrictive temperature of 29°C. A representative leaf from each infection is shown.

Septin-Dependent Assembly of the Exocyst Complex

In *M. oryzae*, the toroidal F-actin network at the appressorium pore is organized by a heteromeric septin ring, composed of septins, Sep3, Sep4, Sep5, and Sep6 (Dagdas et al., 2012). To test whether exocyst assembly at the pore utilizes the F-actin cytoskeleton or microtubules, we added 10 μM latrunculin A (an actin depolymerizing agent), 30 μM benomyl (a microtubule disrupting agent), or 0.1% DMSO (control) to the conidial suspension after 16 h of appressorium development. The exocyst ring was significantly disrupted by latrunculin A treatment ($P < 0.01$, $n = 100$) compared with either benomyl or DMSO (Supplemental Figure 10).

The observed physical interaction between the exocyst complex and septin GTPases suggested a role for septins in exocyst organization (Table 1). Therefore, we decided to test whether septins are required for assembly of the exocyst complex at the appressorium pore. To do this, we expressed Sec6-GFP in a Δ*sep3* mutant. During early stages of appressorium formation (4 h), Sec6p showed cortical localization in a Δ*sep3* mutant as in Guy11. During appressorium maturation, however, Sec6p mislocalized in a Δ*sep3* mutant as shown in Figure 5 and Supplemental Figure 11. Consistent with this, *M. oryzae* septins are only expressed after 8 h of appressorium development (Dagdas et al., 2012), and we observed transition of the exocyst from the cortex of the appressorium to the pore after 11 h of development. When considered together, these observations suggest that the appressorium pore is first defined by septins and that this is necessary for exocyst organization (Supplemental Figure 12 and Supplemental Movie 6).

CHM1 is a Cla4 homolog of yeast in *M. oryzae* and a member of the PAK (p21-activated kinase) family that phosphorylates septins. In *M. oryzae*, the Δ*chm1* mutant is not able to form either a septin ring or the toroidal F-actin network (Dagdas et al., 2012). We observed Sec6:GFP in a Δ*chm1* mutant and it localized to the cortex of the appressorium at 4 h but was mislocalized in mature appressoria, failing to organize at the pore (Figures 5A and 5B; Supplemental Figure 11).

Exocyst Assembly Requires Regulated Synthesis of Reactive Oxygen Species

Septin-mediated plant infection depends on regulated synthesis of reactive oxygen species (ROS) by NADPH oxidases (Ryder et al., 2013). To test whether organization of the exocyst complex is also dependent on NADPH oxidase activity, we expressed Sec6-GFP in Δ*noxR*, Δ*nox1*, and Δ*nox2* mutants (Ryder et al., 2013). We found that Sec6-GFP was mislocalized in mature appressoria of Δ*noxR* and Δ*nox2* mutants (Figures 5A and 5B; Supplemental Figures 11 and 13). However, in a Δ*nox1* mutant, Sec6-GFP localized in the same way as in the wild-type strain Guy11 (Supplemental Figure 13). This is consistent with the observations made by Ryder et al. (2013), which showed that the NoxR-Nox2 NADPH oxidase is required for septin ring formation at the appressorium pore.

In *M. oryzae*, the Pmk1 pathway is regulated through upstream components, including the MAPK kinase kinase Mst11, MAPK kinase Mst7, and an adaptor protein, Mst50 (Zhao et al., 2005; Park et al., 2006; Wilson and Talbot, 2009). The adaptor protein, Mst50, directly interacts with Cdc42 and the Ras2 GTPase,

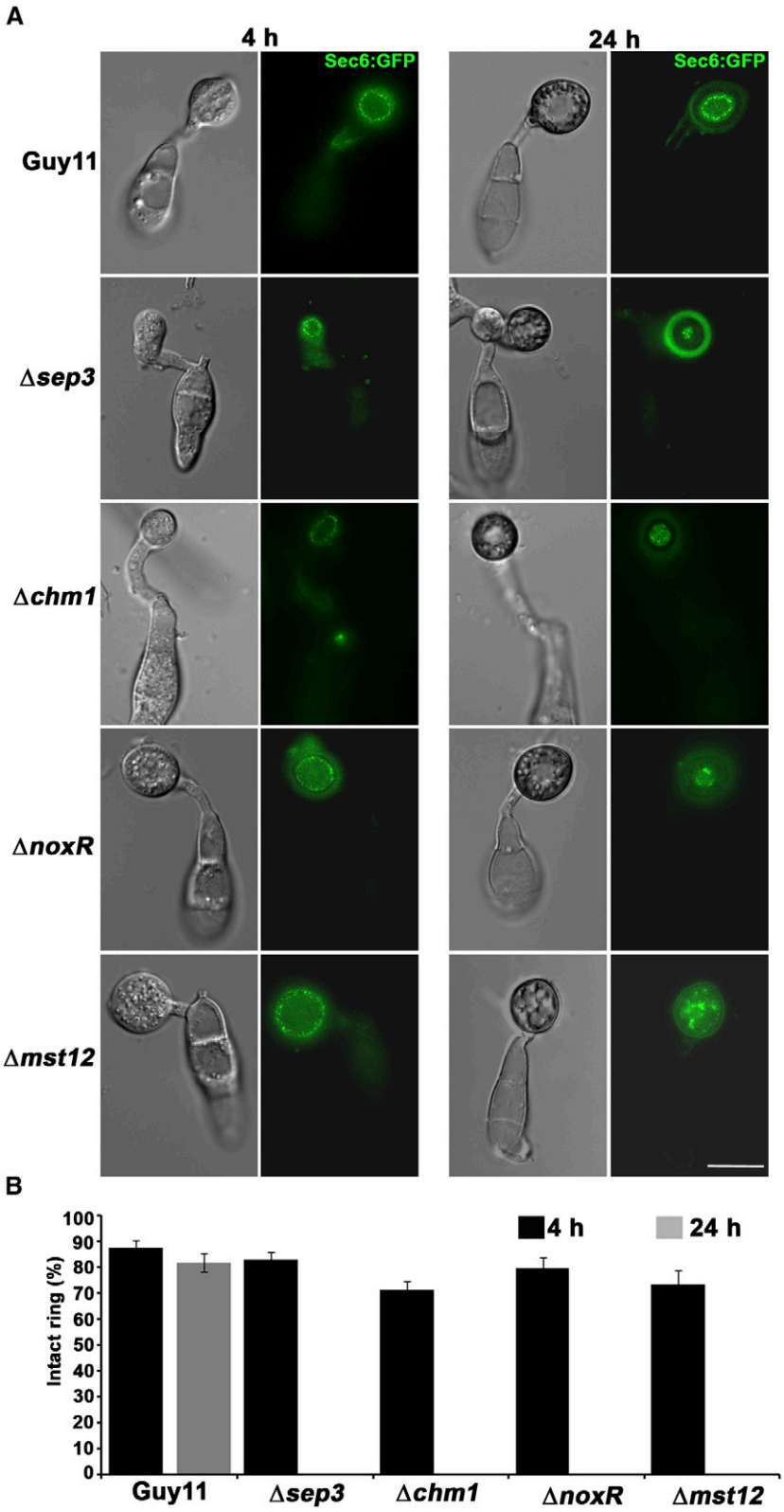

Figure 5. Recruitment of the Exocyst Complex to the Appressorium Pore Is Septin-Dependent.

suggesting that the Pmk1 pathway might be involved in the establishment of cell polarity (Park et al., 2006). We therefore decided to investigate Sec6 localization in a Δ*mst12* mutant. *MST12* encodes a transcription factor that acts downstream of the Pmk1 MAPK pathway of *M. oryzae* and is required for septin ring formation and plant infection (Park et al., 2002; Dagdas et al., 2012). Sec6-GFP was completely mislocalized in mature appressoria of a Δ*mst12* mutant (Figure 5; Supplemental Figure 11). Consistent with this result, Sec6 and Exo84 coimmunoprecipitated both the Mst7 MAPK kinase and Pmk1 MAPK, suggesting an association with this signaling pathway. We conclude that septin assembly, which requires regulated synthesis of ROS and the action of the Pmk1 MAPK pathway, is necessary for organization and maintenance of the exocyst at the base of the appressorium during plant infection.

DISCUSSION

In this study, we set out to understand how polarized exocytosis is regulated during appressorium-mediated infection by the rice blast fungus *M. oryzae*. Appressorium infection of rice plants involves generation of cell polarity so that a penetration hypha can form at the base of the infection cell, to rupture the rice cuticle, and invade the underlying rice tissue. Repolarization of the appressorium is therefore likely to involve remodeling of the secretory apparatus to facilitate the morphogenetic changes required for plant infection. Furthermore, fungal pathogens deliver a large repertoire of effector proteins into host plant cells, requiring rapid and focused secretion, and little is currently understood about this process (Kleemann et al., 2012; Giraldo et al., 2013; Irieda et al., 2014). We therefore characterized the exocyst complex of *M. oryzae*, and based on the analysis reported here, we can make three major conclusions.

First of all, we can conclude that the exocyst forms a complex at the tips of growing hyphae, which can be visualized as a crescent-shape at the apex of the tip, in close proximity to, or associated with, the apical plasma membrane. Exocyst proteins are hydrophilic, cytosolic proteins that can associate with membranes (Terbush et al., 2001), consistent with such a location. Our coimmunoprecipitation experiments, meanwhile, confirmed that the exocyst exists as an octameric complex. The exocyst therefore occupies a distinct site from the vesicle supply center, or Spitzenkörper, which delivers secretory vesicles to the growing tip, consistent with its role in tethering secretory vesicles to the plasma membrane before their SNARE-dependent fusion and cargo deposition (Novick et al., 1981; TerBush et al., 1996). Exocyst localization in *M. oryzae* is similar to that observed in other filamentous fungi, such as *Aspergillus nidulans*, in which the Sec3 homolog SecC is also found in an anterior position to the Spitzenkörper (Taheri-Talesh et al., 2008), and *Candida albicans* (Jones and Sudbery, 2010), where the exocyst complex is located in a crescent tip structure. However, our findings are distinct from exocyst organization in *N. crassa*, where the complex occupies two locations, with Sec5, Sec6, Sec8, and Sec15 localizing as a crescent at the hyphal tip, while Exo70 and Exo84 closely associate with the outer layer of the Spitzenkörper (Riquelme et al., 2014). Such differences may be associated with hyphal growth dynamics, since in *Ashbya gossypii*, AgSec3, AgSec5, and AgExo70 localize to the tips of slow-growing hyphae, but to the Spitzenkörper in faster-growing cells (Köhli et al., 2008). Our observation also revealed a highly dynamic and structured tip growth apparatus in *M. oryzae*, with close association of the exocyst with the t-SNARE Sec9 and the Sec4 Rab GTPase and clear separation from Spitzenkörper-associated proteins, such as Mlc1 and the polarisome component Spa2, as well as a clearly defined subapical endocytic collar region defined by Fimbrin-GFP localization.

The second major conclusion we can make is that the appressorium pore is the site at which the exocyst assembles prior to plant infection, indicating that polarized exocytosis is required for generation of polarity and protrusion of the penetration peg into plant tissue. At the initial stages of appressorium development, the *M. oryzae* exocyst shows cortical distribution at the periphery of the appressorium during its radial expansion and turgor generation. Exocyst distribution then changes in a dynamic manner to the base of the appressorium and the distinct appressorium pore from which polar growth is initiated. Analysis of *Δexo70*, *Δsec5*, and the conditional $Sec6^{Y601P}$ mutants all point to the exocyst complex being important for plant infection, highlighting the requirement for polarized exocytosis at this stage of development, not only for penetration peg emergence, but also for the deployment of virulence-associated proteins. The appressorium pore, however, is also a site of endocytosis, as evidenced by the presence of Fimbrin-GFP and BAR domain proteins such as Rvs167 (Dagdas et al., 2012). Recent evidence suggests that the exocyst may be pivotal to organization of both endocytosis and exocytosis, acting as a network hub for spatial regulation of these interlinked processes (Jose et al., 2015). Our results are consistent with this idea, since endocytosis and exocytosis both occur within the appressorium pore and must be balanced effectively to ensure plasma membrane homeostasis during rapid polarized extension of the penetration peg.

Finally, we can conclude that septins play a key role in recruiting and organizing the exocyst to the appressorium pore. It is clear from temporal analysis of exocyst localization that accumulation at the pore does not occur prior to septin gene expression and ring formation. In *M. oryzae*, septins form a hetero-oligomeric ring around the appressorium pore and Cdc42 is required for ring formation (Dagdas et al., 2012). This is consistent with evidence from budding yeast that deployment of septins to the polarized

Figure 5. (continued).

(A) Micrographs of exocyst subunit Sec6:GFP expressed in wild-type strain Guy11 and Δ*sep3*, Δ*chm1*, Δ*noxR*, and Δ*mst12* mutants. Conidial suspensions at 5×10^4 mL^{-1} were inoculated onto glass cover slips and the expression of Sec6:GFP was checked at 4 and 24 h after inoculation. Bar = 10 μm.
(B) Bar chart showing percentage of appressoria expressing exocyst subunit Sec6:GFP at 4 h (black bars) and 24 h (gray bars) after inoculation. Values are mean ± SD for three repetitions of the experiment, $n = 300$.

bud site is also dependent on Cdc42 and that the septin ring is confined by polarized exocytosis to this region (Okada et al., 2013). In yeast, septins compartmentalize the cortex around the cleavage site and maintain both exocyst and polarisome complexes at the bud site by forming a diffusion barrier (Barral et al., 2000; Dobbelaere and Barral, 2004). In *M. oryzae*, septins act as a diffusion barrier at the appressorium, maintaining the position of proteins such as Tea1, a wide range of BAR domain proteins, and the Arp2/3 complex protein, Las17, associated with actin polymerization, membrane curvature, and repolarization (Dagdas et al., 2012). This study provides evidence that the exocyst complex is also recruited and spatially organized at the appressorium pore in a septin-dependent manner. Consistent with this idea, the regulated synthesis of ROS, which is required for septin ring formation (Ryder et al., 2013), is also necessary for exocyst recruitment, while the interaction between septins and exocyst components predicted by coimmunoprecipitation is also consistent with their close association.

In summary, septin-dependent assembly of the exocyst complex is key to the operation of the specialized infection cell used by the rice blast fungus to gain entry to its host plant. This study is part of an emerging picture of a dynamic infection process that requires integration of diverse signals from the plant to enable a turgor-driven infection process requiring rapid repolarization of the appressorium to facilitate cuticle rupture and entry into rice cells. Being able to target the initial stages of plant infection in such a devastating pathogen is likely to be an effective means of ultimately controlling rice blast disease.

METHODS

Fungal Strains, Growth Conditions, and DNA Analysis

All *Magnaporthe oryzae* isolates used in this study were derived from the wild-type strain Guy11 (Leung et al., 1988). Growth conditions and maintenance of *M. oryzae*, fungal transformation, nucleic acid extraction, and appressorium development assays were performed as previously described (Talbot et al., 1993). Standard procedures were followed for PCR (see Supplemental Table 2 for all primers used), gel electrophoresis, restriction digestion, DNA gel blots, and DNA sequencing (Sambrook and Russell, 2000).

Plant Infection Assay

Rice (*Oryza sativa*) infection assays were performed using the blast-susceptible cultivar CO-39. Spores were harvested from 10- to 12-d-old cultures in sterile distilled water and washed twice. A spore suspension was prepared at 5×10^4 spores mL^{-1} in 0.2% gelatin and sprayed onto 21-d-old rice seedlings using an artist's airbrush. After spray inoculation, plants were kept in plastic bags for 48 h to maintain high humidity and then transferred to a plant growth chamber. Plants were incubated for 5 to 6 d at 24°C with a 12-h light-dark cycle and disease symptoms were analyzed (Talbot et al., 1993). All infection assays were repeated three times using 40 seedlings per experiment.

Light and Epifluorescence Microscopy

Appressorium development assays were performed on hydrophobic boroslicate glass cover slips (Fisher Scientific), as described previously (Ryder et al., 2013). For epifluorescence microscopy, conidia were incubated on cover slips and observed at each time point using an IX-81 inverted microscope (Olympus) and a UPlanSApo ×100/1.40 oil objective. Movies were captured using Zeiss LSM510 Meta and Leica SP8 confocal laser scanning microscope systems. Argon (488-nm laser line) and helium-neon (543-nm laser line) lasers were used to excite GFP and RFP fluorochromes, respectively, and images were recorded under ×63 (Zeiss) or ×40 (Leica) oil immersion objective lenses. All microscopy images were analyzed using MetaMorph (Molecular Devices), LSM Image Browser (Zeiss), or LAS AF (Leica) software. Fluorescence recovery after photobleaching experiments, shown in Supplemental Movie 6, were performed using a Leica SP8 confocal microscope, with an argon laser line (488 nm) to excite GFP for imaging and a 405-nm diode laser to perform photobleaching. Five prebleach scans and 100 postbleach scans were captured at 1-s intervals.

Generation of GFP Fusion Plasmids

All translational GFP-fused constructs were generated by the gap repair cloning method, based on homologous recombination in *Saccharomyces cerevisiae* (Raymond et al., 1999) using primers shown in Supplemental Table 2. Each fragment was amplified and transformed into a *ura3* strain of *S. cerevisiae*. Positive clones were confirmed by colony PCR and used for plasmid extraction. Schematic diagrams for construction of C- and N-terminal translational fusions are shown in Supplemental Figure 10. In each case, primers contain a 30-bp 5′ overlap with adjoining fragments to allow assembly of fragments by homologous recombination. Similarly, the forward primer (Sur.Vec-F) of the sulphonylurea resistance gene cassette (ILV1) (Sweigard et al., 1997) and the reverse primer (TrpC.Vec-R) of the terminator have 30-bp overhangs complementary to the vector sequence (Supplemental Figure 14). N-terminal translational fusions were generated through cloning of the GFP fragment between the native promoter and coding sequence of the corresponding gene (Supplemental Figure 14A). To generate C-terminal translational GFP fusions, primers were designed to amplify the gene of interest including 2 kb upstream of the start codon, GFP, and the TrpC terminator (Supplemental Figure 14B).

Generation of the *M. oryzae sec6*^{Y601P} Temperature-Sensitive Mutant

A temperature-sensitive *sec6* mutant was generated by point mutation at position Y601P of *SEC6*, based on the previously reported *S. cerevisiae* mutation (L633P), which caused temperature sensitivity (Lamping et al., 2005). In *M. oryzae*, we mutated the same conserved region of Sec6p (Supplemental Figure 5A). The hygromycin resistance cassette (Carroll et al., 1994) was cloned between the coding sequence and terminator of the gene. Restriction sites *Bam*HI and *Hin*dIII were introduced into Sec6.TS.1F and Sec6.TER.R primers, respectively (Supplemental Table 2). The plasmid was confirmed by DNA sequencing and a *Bam*HI-*Hin*dIII fragment was used for transformation of Guy11. Allelic replacement mutants were selected and checked by colony PCR and DNA gel blot analysis.

FM4-64 Staining and Treatment with Chemical Inhibitors

FM4-64 solution was prepared as described previously (Bolte et al., 2004). A plug of *M. oryzae* mycelium was inoculated on a water agar slide. After 24 h, a 10 μM aqueous solution of FM4-64 was used to stain vegetative hyphae and then incubated for 5 min, before viewing by epifluorescence microscopy. The microtubule-disrupting agent methyl 1-(butylcarbamoyl)-2-benzimidazolecarbamate (benomyl; Fluka) was used at 30 μM (stock: 10 mM in DMSO) and the actin inhibitor latrunculin A (Enzo Life Sciences) was used at 10 μM (stock: 20 mM in DMSO). Inhibitors were added after 16 h of appressorium development and observations made after 24 h of exposure. DMSO (0.1%) was used as the control treatment.

Protein Secretion Assay

M. oryzae mycelium was prepared by growth in liquid CM for 48 h, harvested by filtration through Miracloth (Calbiochem) and an equal amount of mycelium transferred to liquid GMM for 24 h. Culture filtrates were collected and subsequently freeze-dried. Lyophilized culture filtrate was resuspended, diluted, and assayed using the Bradford method (Bradford, 1976). Protocol and reagents were obtained from Bio-Rad (Quick Start Bradford Kit 2).

Coimmunoprecipitation Experiments and LC-MS/MS Analysis

Total protein was extracted from lyophilized *M. oryzae* mycelium after growth in liquid CM for 48 h and snap frozen in liquid nitrogen. *M. oryzae* strains expressing Sec6:GFP, Exo84:GFP, and ToxA:GFP (control) were coimmunoprecipitated using the GFP-Trap protocol according to the manufacturer's protocol (ChromoTek). Preparation of peptides for LC-MS/MS was performed as follows. Proteins were separated by SDS/PAGE. Gels were cut into slices (~5 Å to ~10 mm) and proteins contained in gel slices prepared for LC-MS/MS, as described previously (Ntoukakis et al., 2009). LC-MS/MS analysis was performed with a LTQ-Orbitrap mass spectrometer (Thermo Scientific) and a nanoflow-HPLC system (nanoACQUITY; Waters) described previously (Oh et al., 2009) with the following differences: MS/MS peak lists were exported in Mascot generic file format using Discoverer v2.2 (Thermo Scientific). The database was searched with Mascot v2.3 (Matrix Science) with the following differences: (1) The database searched with Mascot v2.3 (Matrix Science) was against the *M. oryzae* protein database with the inclusion of sequences of common contaminants such as keratins and trypsin. (2) Carbamidomethylation of cysteine residues was specified as a fixed modification, and oxidized methionine was allowed as a variable modification. Other Mascot parameters used were as follows: (1) Mass values were monoisotopic, and the protein mass was unrestricted. (2) The peptide mass tolerance was 5 ppm, and the fragment mass tolerance was ± 0.6 D. (3) Two missed cleavages were allowed with trypsin. All Mascot searches were collated and verified with Scaffold (Proteome Software), and the subset database was searched with X Tandem (The Global Proteome Machine Organization Proteomics Database and Open Source Software; www.thegpm.org). Accepted proteins passed the following threshold in Scaffold: 95% confidence for protein match and minimum of two unique peptide matches with 95% confidence.

Accession Numbers

Accession numbers for *EXO70*, *SEC6*, *SEC10*, and *SEC15* are KJ606327, KJ606328, KJ606329, and KJ606330, respectively.

Supplemental Data

Supplemental Figure 1. Relative transcript abundance of the exocyst subunit-encoding genes in mycelium and during appressorium development.

Supplemental Figure 2. High-resolution epifluorescence micrograph of Sec3-GFP and FM4-64-labeled Spitzenkörper in vegetative hyphae of *Magnaporthe oryzae*.

Supplemental Figure 3. Localization of Sec2-GFP and FM4-64-labeled Spitzenkörper in vegetative hyphae of *Magnaporthe oryzae.*

Supplemental Figure 4. Localization of polarized secretory apparatus in growing vegetative hyphae.

Supplemental Figure 5. Exocyst localization during a time course of appressorium development in *M. oryzae*.

Supplemental Figure 6. Localization of polarity determinants in the *M. oryzae* appressorium.

Supplemental Figure 7. Quantification of secreted protein from culture filtrates of exocyst mutants.

Supplemental Figure 8. Generation of the *sec6*^{Y601P} temperature-sensitive mutant.

Supplemental Figure 9. Expression and localization of Exo70:GFP, Exo84:GFP, Sec15:GFP, and Sec3:GFP in the *sec6*^{Y601P} mutant.

Supplemental Figure 10. The F-actin cytoskeleton is required for exocyst ring formation at the appressorium pore.

Supplemental Figure 11. Sec6:GFP localization in Δ*sep3*, Δ*noxR*, and Δ*mst12* mutants of *M. oryzae.*

Supplemental Figure 12. Transition of the exocyst from the cortex of the appressorium to the appressorial pore during maturation.

Supplemental Figure 13. Sec6:GFP localization in Δ*nox1* and Δ*nox2* mutants of *M. oryzae.*

Supplemental Figure 14. Schematic diagram to show cloning methodology for each GFP fusion construct.

Supplemental Table 1. List of genes characterized in this study.

Supplemental Table 2. Primers used in this study.

Supplemental Movie 1. Polarisome component Spa2 localizes as a bright spot at the growing tip of the hypha.

Supplemental Movie 2. Fim1:GFP shows cortical actin patches at the subapical region of the growing hyphae.

Supplemental Movie 3. GFP-Cdc42 localizes to the tip of the growing hypha.

Supplemental Movie 4. The v-SNARE Snc1 actively localizes to the tip of the growing hypha.

Supplemental Movie 5. Three-dimensional rotational movie of exocyst subunit Sec6 localized at the base of the appressorium after 24 h.

Supplemental Movie 6. Transition of the exocyst from the cortex of the appressorium to the appressorial pore during maturation, following photobleaching.

ACKNOWLEDGMENTS

This work was funded by a Halpin Scholarship in Rice Blast Research to Y.K.G. and a European Research Council, Advanced Investigator Award to N.J.T. under the European Union's Seventh Framework Programme (*FP7/2007-2013)*/ERC grant agreement 294702 GENBLAST. We thank Peter Novick and Wei Guo for providing yeast strains. We gratefully acknowledge bioinformatics support of Darren M. Soanes and technical support from Barbara Saddler.

AUTHOR CONTRIBUTIONS

N.J.T., Y.K.G., and Y.F.D. designed the research. Y.K.G., Y.F.D., A.-L.M.-R., M.J.K., and G.R.L. executed the experiments. J.S. and F.M. carried out mass spectrometry analysis of the exocyst complex. N.J.T. and Y.K.G. wrote the article.

Received June 19, 2015; revised October 5, 2015; accepted October 20, 2015; published November 13, 2015.

REFERENCES

Barral, Y., Mermall, V., Mooseker, M.S., and Snyder, M. (2000). Compartmentalization of the cell cortex by septins is required for maintenance of cell polarity in yeast. Mol. Cell **5:** 841–851.

Bolte, S., Talbot, C., Boutte, Y., Catrice, O., Read, N.D., and Satiat-Jeunemaitre, B. (2004). FM-dyes as experimental probes for dissecting vesicle trafficking in living plant cells. J. Microsc. **214:** 159–173.

Bradford, M.M. (1976). A rapid and sensitive method for the quantitation of microgram quantities of protein utilizing the principle of protein-dye binding. Anal. Biochem. **72:** 248–254.

Carroll, A., Sweigard, J., and Valent, B. (1994). Improved vectors for selecting resistance to hygromycin. Fungal Genet. Newsl. **41:** 22.

Dagdas, Y.F., Yoshino, K., Dagdas, G., Ryder, L.S., Bielska, E., Steinberg, G., and Talbot, N.J. (2012). Septin-mediated plant cell invasion by the rice blast fungus, *Magnaporthe oryzae.* Science **336:** 1590–1595.

Dean, R.A., et al. (2005). The genome sequence of the rice blast fungus *Magnaporthe grisea.* Nature **434:** 980–986.

de Jong, J.C., McCormack, B.J., Smirnoff, N., and Talbot, N.J. (1997). Glycerol generates turgor in rice blast. Nature **389:** 244–245.

Dobbelaere, J., and Barral, Y. (2004). Spatial coordination of cytokinetic events by compartmentalization of the cell cortex. Science **305:** 393–396.

Evangelista, M., Zigmond, S., and Boone, C. (2003). Formins: signaling effectors for assembly and polarization of actin filaments. J. Cell Sci. **116:** 2603–2611.

Fischer-Parton, S., Parton, R.M., Hickey, P.C., Dijksterhuis, J., Atkinson, H.A., and Read, N.D. (2000). Confocal microscopy of FM4-64 as a tool for analysing endocytosis and vesicle trafficking in living fungal hyphae. J. Microsc. **198:** 246–259.

Giraldo, M.C., Dagdas, Y.F., Gupta, Y.K., Mentlak, T.A., Yi, M., Martinez-Rocha, A.L., Saitoh, H., Terauchi, R., Talbot, N.J., and Valent, B. (2013). Two distinct secretion systems facilitate tissue invasion by the rice blast fungus *Magnaporthe oryzae.* Nat. Commun. **4:** 1996.

Giraldo, M.C., and Valent, B. (2013). Filamentous plant pathogen effectors in action. Nat. Rev. Microbiol. **11:** 800–814.

Guo, W., Grant, A., and Novick, P. (1999). Exo84p is an exocyst protein essential for secretion. J. Biol. Chem. **274:** 23558–23564.

Hamer, J.E., Howard, R.J., Chumley, F.G., and Valent, B. (1988). A mechanism for surface attachment in spores of a plant pathogenic fungus. Science **239:** 288–290.

He, B., and Guo, W. (2009). The exocyst complex in polarized exocytosis. Curr. Opin. Cell Biol. **21:** 537–542.

Irieda, H., Maeda, H., Akiyama, K., Hagiwara, A., Saitoh, H., Uemura, A., Terauchi, R., and Takano, Y. (2014). *Colletotrichum orbiculare* secretes virulence effectors to a biotrophic interface at the primary hyphal neck via exocytosis coupled with SEC22-mediated traffic. Plant Cell **26:** 2265–2281.

Jones, L.A., and Sudbery, P.E. (2010). Spitzenkorper, exocyst, and polarisome components in *Candida albicans* hyphae show different patterns of localization and have distinct dynamic properties. Eukaryot. Cell **9:** 1455–1465.

Jose, M., Tollis, S., Nair, D., Mitteau, R., Velours, C., Massoni-Laporte, A., Royou, A., Sibarita, J-B., and McCusker, D. (2015). A quantitative imaging-based screen reveals the exocyst as a network hub connecting endocytosis and exocytosis. Mol. Biol. Cell **26:** 2519–2534.

Kershaw, M.J., and Talbot, N.J. (2009). Genome-wide functional analysis reveals that infection-associated fungal autophagy is necessary for rice blast disease. Proc. Natl. Acad. Sci. USA **106:** 15967–15972.

Khang, C.H., Berruyer, R., Giraldo, M.C., Kankanala, P., Park, S.Y., Czymmek, K., Kang, S., and Valent, B. (2010). Translocation of *Magnaporthe oryzae* effectors into rice cells and their subsequent cell-to-cell movement. Plant Cell **22:** 1388–1403.

Kleemann, J., Rincon-Rivera, L.J., Takahara, H., Neumann, U., Ver Loren van Themaat, E., van der Does, H.C., Hacquard, S., Stüber, K., Will, I., Schmalenbach, W., Schmelzer, E., and O'Connell, R.J. (2012). Sequential delivery of host-induced virulence effectors by appressoria and intracellular hyphae of the phytopathogen *Colletotrichum higginsianum.* PLoS Pathog. **8:** e1002643.

Köhli, M., Galati, V., Boudier, K., Roberson, R.W., and Philippsen, P. (2008). Growth-speed-correlated localization of exocyst and polarisome components in growth zones of *Ashbya gossypii* hyphal tips. J. Cell Sci. **121:** 3878–3889.

Lamping, E., Tanabe, K., Niimi, M., Uehara, Y., Monk, B.C., and Cannon, R.D. (2005). Characterization of the *Saccharomyces cerevisiae* sec6-4 mutation and tools to create S. cerevisiae strains containing the sec6-4 allele. Gene **361:** 57–66.

Leung, H., Borromeo, S., Bernardo, M.A., and Notteghem, J.L. (1988). Genetic analysis of virulence in the rice blast fungus *Magnaporthe grisea.* Phytopathology **78:** 1227–1233.

Novick, P., Ferro, S., and Schekman, R. (1981). Order of events in the yeast secretory pathway. Cell **25:** 461–469.

Novick, P., Field, C., and Schekman, R. (1980). Identification of 23 complementation groups required for post-translational events in the yeast secretory pathway. Cell **21:** 205–215.

Novick, P., Medkova, M., Dong, G., Hutagalung, A., Reinisch, K., and Grosshans, B. (2006). Interactions between Rabs, tethers, SNAREs and their regulators in exocytosis. Biochem. Soc. Trans. **34:** 683–686.

Ntoukakis, V., Mucyn, T.S., Gimenez-Ibanez, S., Chapman, H.C., Gutierrez, J.R., Balmuth, A.L., Jones, A.M.E., and Rathjen, J.P. (2009). Host inhibition of a bacterial virulence effector triggers immunity to infection. Science **324:** 784–787.

Oh, S.-K., et al. (2009). *In planta* expression screens of *Phytophthora infestans* RXLR effectors reveal diverse phenotypes, including activation of the *Solanum bulbocastanum* disease resistance protein Rpi-blb2. Plant Cell **21:** 2928–2947.

Okada, S., Leda, M., Hanna, J., Savage, N.S., Bi, E., and Goryachev, A.B. (2013). Daughter cell identity emerges from the interplay of Cdc42, septins, and exocytosis. Dev. Cell **26:** 148–161.

Park, G., Xue, C., Zhao, X., Kim, Y., Orbach, M., and Xu, J.R. (2006). Multiple upstream signals converge on the adaptor protein Mst50 in *Magnaporthe grisea.* Plant Cell **18:** 2822–2835.

Park, G., Xue, C., Zheng, L., Lam, S., and Xu, J.R. (2002). MST12 regulates infectious growth but not appressorium formation in the rice blast fungus *Magnaporthe grisea.* Mol. Plant Microbe Interact. **15:** 183–192.

Raymond, C.K., Pownder, T.A., and Sexson, S.L. (1999). General method for plasmid construction using homologous recombination. Biotechniques **26:** 134–138, 140–131.

Read, N.D. (2011). Exocytosis and growth do not occur only at hyphal tips. Mol. Microbiol. **81:** 4–7.

Riquelme, M. (2013). Tip growth in filamentous fungi: a road trip to the apex. Annu. Rev. Microbiol. **67:** 587–609.

Riquelme, M., Bartnicki-García, S., González-Prieto, J.M., Sánchez-León, E., Verdín-Ramos, J.A., Beltrán-Aguilar, A., and Freitag, M. (2007). Spitzenkorper localization and intracellular traffic of green fluorescent protein-labeled CHS-3 and CHS-6 chitin synthases in living hyphae of *Neurospora crassa.* Eukaryot. Cell **6:** 1853–1864.

Riquelme, M., Bredeweg, E.L., Callejas-Negrete, O., Roberson, R.W., Ludwig, S., Beltrán-Aguilar, A., Seiler, S., Novick, P., and Freitag, M. (2014). The *Neurospora crassa* exocyst complex tethers Spitzenkörper vesicles to the apical plasma membrane during polarized growth. Mol. Biol. Cell **25:** 1312–1326.

Ryder, L.S., Dagdas, Y.F., Mentlak, T.A., Kershaw, M.J., Thornton, C.R., Schuster, M., Chen, J., Wang, Z., and Talbot, N.J. (2013). NADPH oxidases regulate septin-mediated cytoskeletal remodeling during plant infection by the rice blast fungus. Proc. Natl. Acad. Sci. USA **110:** 3179–3184.

Sagot, I., Klee, S.K., and Pellman, D. (2002). Yeast formins regulate cell polarity by controlling the assembly of actin cables. Nat. Cell Biol. **4:** 42–50.

Salminen, A., and Novick, P.J. (1989). The Sec15 protein responds to the function of the GTP binding protein, Sec4, to control vesicular traffic in yeast. J. Cell Biol. **109:** 1023–1036.

Sambrook, J., and Russell, D.W. (2000). Molecular Cloning: A Laboratory Manual. (Cold Spring Harbor, NY: Cold Spring Harbor Laboratory Press).

Saunders, D.G.O., Aves, S.J., and Talbot, N.J. (2010). Cell cycle-mediated regulation of plant infection by the rice blast fungus. Plant Cell **22:** 497–507.

Sheu, Y.J., Santos, B., Fortin, N., Costigan, C., and Snyder, M. (1998). Spa2p interacts with cell polarity proteins and signaling components involved in yeast cell morphogenesis. Mol. Cell. Biol. **18:** 4053–4069.

Soanes, D.M., Chakrabarti, A., Paszkiewicz, K.H., Dawe, A.L., and Talbot, N.J. (2012). Genome-wide transcriptional profiling of appressorium development by the rice blast fungus *Magnaporthe oryzae.* PLoS Pathog. **8:** e1002514.

Songer, J.A., and Munson, M. (2009). Sec6p anchors the assembled exocyst complex at sites of secretion. Mol. Biol. Cell **20:** 973–982.

Stalder, D., Mizuno-Yamasaki, E., Ghassemian, M., and Novick, P.J. (2013). Phosphorylation of the Rab exchange factor Sec2p directs a switch in regulatory binding partners. Proc. Natl. Acad. Sci. USA **110:** 19995–20002.

Steinberg, G. (2007). Hyphal growth: a tale of motors, lipids, and the Spitzenkörper. Eukaryot. Cell **6:** 351–360.

Sudbery, P. (2011a). Fluorescent proteins illuminate the structure and function of the hyphal tip apparatus. Fungal Genet. Biol. **48:** 849–857.

Sudbery, P.E. (2011b). Growth of *Candida albicans* hyphae. Nat. Rev. Microbiol. **9:** 737–748.

Sweigard, J., Chumley, F., Carrol, A., Farrall, L., and Valent, B. (1997). A series of vectors for fungal transformation. Fungal Genet. Newsl. **44:** 52–55.

Taheri-Talesh, N., Horio, T., Araujo-Bazán, L., Dou, X., Espeso, E.A., Peñalva, M.A., Osmani, S.A., and Oakley, B.R. (2008). The tip growth apparatus of *Aspergillus nidulans.* Mol. Biol. Cell **19:** 1439–1449.

Talbot, N.J., Ebbole, D.J., and Hamer, J.E. (1993). Identification and characterization of MPG1, a gene involved in pathogenicity from the rice blast fungus *Magnaporthe grisea.* Plant Cell **5:** 1575–1590.

Terbush, D.R., Guo, W., Dunkelbarger, S., and Novick, P. (2001). Purification and characterization of yeast exocyst complex. Methods Enzymol. **329:** 100–110.

TerBush, D.R., Maurice, T., Roth, D., and Novick, P. (1996). The exocyst is a multiprotein complex required for exocytosis in *Saccharomyces cerevisiae.* EMBO J. **15:** 6483–6494.

Veneault-Fourrey, C., Barooah, M., Egan, M., Wakley, G., and Talbot, N.J. (2006). Autophagic fungal cell death is necessary for infection by the rice blast fungus. Science **312:** 580–583.

Verdín, J., Bartnicki-Garcia, S., and Riquelme, M. (2009). Functional stratification of the Spitzenkörper of *Neurospora crassa*. Mol. Microbiol. **74:** 1044–1053.

Wiederkehr, A., Du, Y., Pypaert, M., Ferro-Novick, S., and Novick, P. (2003). Sec3p is needed for the spatial regulation of secretion and for the inheritance of the cortical endoplasmic reticulum. Mol. Biol. Cell **14:** 4770–4782.

Wilson, R.A., and Talbot, N.J. (2009). Under pressure: investigating the biology of plant infection by *Magnaporthe oryzae*. Nat. Rev. Microbiol. **7:** 185–195.

Xu, J.R., and Hamer, J.E. (1996). MAP kinase and cAMP signaling regulate infection structure formation and pathogenic growth in the rice blast fungus *Magnaporthe grisea*. Genes Dev. **10:** 2696–2706.

Zhao, X., Kim, Y., Park, G., and Xu, J.R. (2005). A mitogen-activated protein kinase cascade regulating infection-related morphogenesis in *Magnaporthe grisea.* Plant Cell **17:** 1317–1329.